Received: 27 September 2023 | Revised: 12 March 2024 | Accepted: 21 April 2024

DOI: 10.1002/app.55652

RESEARCH ARTICLE

Applied Polymer SCIENCE WILEY

A continuous melt extrusion approach toward polyethylene-based vitrimers with improved crosslinking and performance

Subhaprad Ash[1,2] | **Rishi Sharma**[1] | **Muhammad Naveed**[1] | **Shalin Patil**[3] | **Shiwang Cheng**[3] | **Muhammad Rabnawaz**[1,2,3]

[1]School of Packaging, Michigan State University, East Lansing, Michigan, USA

[2]Department of Chemistry, Michigan State University, East Lansing, Michigan, USA

[3]College of Engineering Building, Michigan State University, East Lansing, Michigan, USA

Correspondence
Muhammad Rabnawaz, School of Packaging, Michigan State University, 448 Wilson Road, East Lansing, MI 48824-1223, USA.
Email: rabnawaz@msu.edu

Funding information
National Science Foundation, Grant/Award Number: 2044877

Abstract

Reported herein is a continuous one-step melt extrusion approach for high-density polyethylene (HDPE) vitrimers. A grafting agent and a coagent were used to produce high-performing vitrimers. Maleic anhydride (MA) served as a reactive agent to facilitate crosslinking, while dimethyl maleate (DM) acted as a grafting enhancer by reducing the surface energy of HDPE grafted with MA. For comparison, MA alone was also tested as a grafting agent. The vitrimers obtained displayed superior mechanical properties compared with HDPE. The storage modulus, as well as crystallinity, were determined for the HDPE vitrimers. These vitrimers are reprocessable, thus supporting recycling efforts despite their crosslinked nature, owing to very fast relaxation due to low activation energy for the transesterification reaction. Consequently, these vitrimers are not only recyclable but also exhibit enhanced thermal and mechanical properties compared with conventional HDPE.

KEYWORDS

crosslinking, extrusion, grafting, recycling

1 | INTRODUCTION

Polyethylene (PE) is the most widely used commodity plastic by volume. In particular, high-density polyethylene (HDPE) is in high demand with applications ranging from construction materials to packaging.[1,2] It used to produce many items that have important roles in our daily lives, such as plastic bags, bottles, films, and pipes. HDPE that has been crosslinked to form permanent covalent bonds is known as crosslinked HDPE (XLHDPE). As a result of its crosslinked structure, XLHDPE has enhanced mechanical properties. XLHDPE is often used to produce pipes as well as insulation for high voltage cables.[3] However, XLHDPE is difficult to reprocess due to the presence of these permanent covalent bonds, which impede efforts to recycle and reuse this material.

Vitrimers are emerging as a new class of materials that will open the possibility to transform commodity thermoplastics into high performance materials.[4–16] They are an example of associative covalent adaptable networks (CANs) in which exchange reactions occur without causing changes in the crosslinking density and they do not exhibit depolymerization upon heating.[17–22] Therefore, the cleavage of one bond in a CAN is

accompanied by the formation of another bond, which replaces it. Vitrimers were first developed with epoxy/acid or epoxy/anhydride polyester-based networks using a transesterification catalyst.[23] As is the case with vitreous silica, thermally triggered catalytic transesterification reactions yield permanent polyester/polyol networks with viscosities that gradually decrease upon heating.[24]

Transesterification is a popular approach for the modification of PE-based vitrimers.[23] For example, Leibler and coworkers.[23,25] and Terentjev and coworkers[26] used a free-radical initiator to produce maleated polypropylene (MA-PP) and maleated polyethylene (MA-PE) through reactive extrusion that was further crosslinked with bifunctional epoxide in the presence of a catalyst. This study also explored the effect of crosslinker density and maleic anhydride (MA) grafting density on the performance of PP- and PE-vitrimers and showed the critical role of the catalyst on vitrimeric behavior. In 2017, Röttger et al. also reported high-performance vitrimers by using metathesis of dioxaborolanes.[25] Two different methodologies were applied to generate vitrimers. In the first method, copolymers containing dioxaborolanes were synthesized from monomers of poly(methyl methacrylate) and polystyrene. In the second method, dioxaborolanes were grafted onto HDPE by reactive extrusion processing. Crosslinking was achieved in both cases by means of metathesis reactions with bis-dioxaborolanes. Nicolaÿ and coworkers used TEMPO-assisted nitroxide chemistry to radically graft bis-boronic esters and took advantage of boronic ester metathesis to create HDPE vitrimers by reactive extrusion.[27] The advantage of nitroxide-mediated grafting is that it prevents permanent crosslinking caused by combination of macroradicals. There have been some studies related to reprocessable PE vitrimers that have been synthesized in one-pot using solvent free method of reactive extrusion. For example, PE vitrimers using di-maleimide bis-dioxaborolane with different spacer alkyl groups has been reported.[28] Here, the researchers highlight the importance of miscibility of grafting agents into molten PE in order to achieve good grafting and thereby enhanced mechanical properties. Therefore, understanding the surface properties that lead to compatibility between the polymers and grafting agents needs to be studied. In another study, MA grafted onto Linear-low density polyethylene (LLDPE) that had been crosslinked by 4,4′-dithiodianiline was created that showed decreased crystallinity as well as improved storage modulus and dimensional stability retaining the elastic behavior.[29] Also, HDPE vitrimers exhibited less warpage and improved interlayer adhesion when they were subjected to 3D printing.[30] In yet another study, the researchers claimed that the yield strength and stiffness of PE vitrimers decreased with increased crosslinking but that also led to decrease in crystallinity.[31]

A key roadblock preventing HDPE vitrimers from achieving high crosslinking density and hence better mechanical performance at higher temperature is the low grafting density of MA onto HDPE. In addition, heterogeneous modification along with side-reactions, such as the homopolymerization of the grafting agents and crosslinking of the HDPE polymers are other challenges. One possible reason for the poor grafting of MA onto HDPE could be the mismatch between the surface energies (SEs) of HDPE (a nonpolar polymer with a SE of 36 mN m^{-1}) with that of MA. It is noteworthy that MA has a high SE as evidenced from the fact that polypropylene (PP) has SE of 30 mJ m^{-2} (or mN m^{-1} and dynes cm^{-1}) and PP with MA grafting density of only 1.5 wt% has a SE of 38 mJ m^{-2}.[32] This SE mismatch between polar grafting agents (e.g., MA) and nonpolar polymers (HDPE and PP) during reactive extrusion processing leads to poor melt miscibility. For example, diols induce phase separation in PE grafted with bis-dioxaborolanes, thereby making it difficult for the system to undergo transesterification.[25] Moreover, MA forms succinic anhydride oligomers along with the occurrence of other side-reactions in PP and PE such as chain scission and self-crosslinking.[33] Therefore, the research gap in SE mismatch needs to be addressed.

The main aim of this research is to decrease the SE of the PE after grafting and create reprocessable vitrimers via one-step. Herein, we report the use of MA and diepoxy crosslinkers for HDPE vitrimers. The novelty of this work is that we explored the effect of DM as a grafting coagent in an attempt to overcome the mismatch in the SEs because DM has a wetting tension of 38.1 dynes cm^{-1} due to the two dangling methyl groups. The use of DM with a SE matching that of HDPE is likely to promote the grafting of MA onto HDPE and thus yield HDPE vitrimers with improved performance thanks to their higher crosslinking densities. Moreover, these vitrimers are reprocessable while retaining their desirable mechanical properties (high stiffness and tensile strength). A key benefit of our approach is that it employs a continuous one-pot method that produces vitrimers with enhanced properties.

2 | EXPERIMENTAL

2.1 | Materials and methods

High-density polyethylene (HDPE, DOWLEX™ IP 10262)[34] with a melt flow index (MFI) = 9 g/10 min at

(190°C, 2.16 kg) was obtained from Dow Chemical, USA. Maleic anhydride (MA, 99%), dimethyl maleate (DM, 96%), 1,4-butanediol diglycidyl ether (≥95%), dicumyl peroxide (DCP, 98%), and zinc acetylacetonate hydrate (99.995% trace metals basis) were purchased from Sigma Aldrich, Milwaukee, WI. All these materials were used as received without further purification. A summary of the codes or abbreviations of the materials used along with their roles in this study is given in Table 1.

2.2 | General procedure for the one-step continuous synthesis of the vitrimers

A summary of the HDPE vitrimers of varied compositions prepared in this study is provided in Table 2. All chemicals were initially physically mixed and subsequently fed as a single dose to a DSM Xplore 15cc Micro Extruder equipped with corotating conical twin-screws that rotated at 100 rpm, where the reaction continued for 4 min at 190°C. Extruded samples were then injection molded in an Xplore injection molder IM5.5#0802 at 190°C to create samples for tensile, impact, and dynamic mechanical analysis (DMA). The mold temperature of the injection molding machine was maintained at 85°C. The pressure used to inject the molten material was 6.0 bar.

TABLE 1 A list of material codes and their function used in the study.

Material	Code	Function
High-density polyethylene	HDPE	Polymer
Maleic anhydride	MA	Grafting agent
Dimethyl maleate	DM	Cografting agent
Dicumyl peroxide	DCP	Initiator
1,4-Butanediol diglycidyl ether	Al	Aliphatic diepoxy crosslinker
Zinc acetylacetonate hydrate	-	Catalyst

2.3 | Differential scanning calorimetry

The thermal properties of HDPE and HDPE-vitrimers were investigated with a TA Instruments Model Q100 differential scanning calorimetry (DSC) system under the continuous flow of nitrogen at a rate of 100 mL min^{-1}. The samples of 7.0 ± 0.5 mg were scraped from three different places on each injection molded sample and kept in aluminum DSC pans with a lid. The study was conducted at a heating rate of 10°C min^{-1} from 25 to 200°C in a nitrogen atmosphere.

2.4 | Thermogravimetric analysis

Thermal characterization of the vitrimers was conducted with a TA Instruments Model Q50 thermogravimetric analysis system. A small quantity of each sample (8.0 ± 0.5 mg) was placed in an aluminum pan. The temperature was then ramped from 25 to 600°C at a heating rate of 10°C min^{-1} under a nitrogen atmosphere with a flow rate of 40 mL min^{-1}.

2.5 | Ultimate tensile testing

Tensile testing was performed after the samples had been aged for 40 h at 23°C using an Instron 5565P6021

TABLE 2 Formulations (mol%) of materials used to produce high-density polyethylene (HDPE) vitrimers.

Sample	Maleic anhydride, MA (mol%)	Dimethyl maleate, DM (mol%)	Dicumyl peroxide, DCP (mol%)	Catalyst (mol%)	Crosslinker, Al (mol%)
HDPE	0	0	0	0	0
$MA_{0.5}$	0.14	0.00	0.01	0.21	0.18
$MA_{0.5}DM_{0.5}$	0.14	0.10	0.01	0.21	0.18
$MA_{0.5}DM_1$	0.14	0.19	0.02	0.21	0.18
MA_1	0.29	0.00	0.01	0.21	0.36
MA_1DM_1	0.29	0.19	0.01	0.21	0.36
MA_2	0.57	0.00	0.02	0.21	0.71
MA_2DM_2	0.57	0.39	0.04	0.21	0.71
DM_1	0	0.29	0.01	0.21	0.36

Note: All the sample names used in this study are designated by the weight percentage of the grafting agent. For example, MA_2DM_2 denotes a sample of HDPE grafted with 2 wt% maleic anhydride (MA) and 2 wt% dimethyl maleate (DM) crosslinked with aliphatic crosslinker (Al).

universal testing machine, USA. The device was equipped with a 5 kN load cell. Tests were performed according to the ASTM D638[35] test procedure. The type V specimens with a respective width, thickness, and gauge length of 3.25, 3.25, and 12.5 mm were tested at an extension rate of 10 mm min^{-1}. Five samples of each composition were studied, and the mean value is reported with standard deviation error.

2.6 | Dynamic mechanic analysis

DMA tests were performed using the tensile configuration on a TA Instruments RSA-G2 instrument, USA. Rectangular specimens obtained via injection molding with dimensions of 12.5 mm × 6.25 mm × 3.25 mm were used. A temperature ramp was conducted in the tensile mode on rectangular specimens at a rate of 2°C min^{-1} and at a frequency of 1 Hz with 0.01% strain from 40 to 220°C for vitrimeric HDPE samples. The temperature range for the control HDPE sample was from 40 to 140°C. Prior to starting the temperature scan, the DMA system was equilibrated at 40°C for 5 min.

2.7 | Impact testing

After initial aging for 40 h at 23°C, Izod impact strength tests were performed on notched specimens with a Ray Ran Test Equipment Ltd instrument, Model RR/IMT (USA), according to the ASTM D256 test method.[36] At least five samples of each composition were studied, and the mean value is reported.

2.8 | Fourier-transform infrared spectroscopy

A Jasco Fourier-transform infrared (FTIR) spectrometer (FTIR-6600 type Easton, MD, USA) equipped with an ATR PRO ONE accessory was used to perform FTIR analysis. For each spectrum, a total of 32 scans was recorded over the wavelength range of 400–4000 cm^{-1}.

2.9 | ^{1}H NMR spectroscopy

A 2-g portion of the MA grafted HDPE was heated in 100 mL of refluxing xylene for 4 h, prior to hot filtration into 300 mL acetone. The xylene-soluble, acetone-insoluble polymer was washed with acetone and dried in vacuo at 60°C. ^{1}H nuclear magnetic resonance (NMR) spectra of this extracted sample were recorded with a Bruker 500 MHz superconducting NMR spectrometer that was equipped with a 10 mm broadband (50–126 MHz) probe. The spectra were recorded at 499.955 MHz and at a temperature of 120°C using 1,1,2,2-tetrachloroethane-d_2 as the solvent.

2.10 | SE calculation

Contact angles and SEs of the HDPE and modified polymers were measured with the help of 590-U1 Advanced Automated Goniometer (Ramé-Hart Instrument Co., NJ, USA). Water and diiodomethane were employed as test liquids for contact angle measurements, and these values were used to calculate total surface energy (TSE) of the polymer samples. The contact angles were measured via DROPimage Advanced software. The SE calculations were calculated from contact angles using Advanced software accounting for the geometric addition of polar and dispersive components.

2.11 | Dyne test inks

Accu Dyne Test™ marker pens acquired from Diversified Enterprises, Claremont, NH, USA with dyne levels of 38, 40, 42, and 44 dynes cm^{-1} were used in this study. The ink was applied to the polymer surface. If the ink beaded up or shrank, a lower dyne level was chosen. If the ink remained on the surface for more than 3 s, a higher dyne level was chosen. The dyne level was defined as the level at which the ink remained for one to 3 s before losing integrity.

2.12 | Melt flow rate

MFRs were determined with RR-6MBA Advanced Melt Flow System (Ray-Ran Test Equipment Ltd., Warwickshire, UK). First, the polymers were allowed to melt for 5 min at 190°C and then subjected to 2.16 kg load at this temperature. MFR values were calculated by taking the weight of sample flowing out of the capillary dye over a span of 10 min.

2.13 | Scanning electron microscopy

Scanning electron microscopy (SEM) analysis was performed on JEOL 7500F system equipped at 5 kV and the images were captured at 5000× magnification. Samples were fractured with a Ray Ran Test Equipment, Model RR/IMT (USA) before analysis.

2.14 | Gel permeation chromatography

High-temperature gel permeation chromatography (GPC) was performed by Milliken Research with an Agilent Technologies PL-GPC 200 instrument. Approximately 15–20 mg of each sample was stabilized in 1,2,4-Trichlorobenzene (TCB) stabilized with 200 mg L^{-1} of BHT at a dissolution temperature of 160°C. Subsequently, 200 μL of sample was injected with a flowrate of 1.0 mL min^{-1} and three Agilent PLgel 13 μm Olexis 300 × 7.5 mm columns were used to analyze the samples.

2.15 | Stress relaxation experiments

Stress relaxation tests were conducted on a TA-ARES instrument. The ARES rheometer is equipped with a Rheometric Scientific Oven for temperature control with an accuracy of ±0.1 K. The stress relaxation measurements were performed using an 8 mm parallel-plate geometry with a thickness of 0.8 mm. After a 10 min temperature equilibration for each temperature from 145 to 165°C (every 5°C), a constant 5% strain was applied, and the stress was monitored over time. According to the strain sweep experiment, 5% deformations were within the linear range.

3 | RESULTS AND DISCUSSION

HDPE vitrimers have been reported in the past, but our goal was to create HDPE-based vitrimers with enhanced mechanical properties like thermosets and which could be melt reprocessed like thermoplastics. The use of MA alone as grafting agent for HDPE leads to phase separation of HDPE-*g*-MA even at lower and nonuniform grafting density and thus prevents higher MA grafting.[25] We hypothesized that to achieve denser grafting, better miscibility would be needed between HDPE and HDPE-*g*-MA during the reaction. To do so, we employed DM as a cografting agent along with MA. DM was selected because its SE matches that of HDPE, and thus it helps to ensure that the SE of MA-grafted HDPE remains closer to that of ungrafted HDPE. This matching SE promotes better miscibility of MA with MA-grafted HDPE, and ultimately increases the overall grafting of MA on HDPE.

The chemistry of our HDPE-vitrimers is shown in Figure 1. First, MA and DM were grafted onto HDPE using DCP as an initiator. Aliphatic diglycidyl ether crosslinker was employed to create crosslinks with HDPE-grafted-MA. Zinc acetylacetonate hydrate facilitated the transesterification reactions at higher temperatures. The addition of MA at concentrations beyond 2 wt% caused the torque to exceed 40 N m, which makes it difficult to melt-process. Therefore, we tested different grafting densities of MA and DM on HDPE by varying the MA and DM contents from 0.5 to 2 wt%. Meanwhile, the mol% ratio of aliphatic diepoxy to MA was kept at 1.25, meaning that for each anhydride site there is an excess of reactive epoxy groups (1.25 times) to facilitate the transesterification reaction.

The distinctive feature of vitrimers is their high storage modulus above the melting temperature of semicrystalline polymer or above the glass temperature (T_g) in the case of fully amorphous polymer. This phenomenon can be studied by looking at the storage modulus in the DMA plot (Figure 2). The plateau after the melting temperature (T_m) suggests the formation of crosslinked HDPE. The storage modulus increased with a higher MA grafting density, indicating that more crosslinking bonds were present. Among the different vitrimers, the highest storage modulus was observed for MA_2DM_2, which was presumably due to uniform and enhanced grafting of MA onto HDPE in this case as compared with that achieved for MA_2 alone. As expected, for non-crosslinked HDPE, the storage modulus loss reached essentially zero after T_m.

Crosslinking density is defined as the number of crosslinks per unit volume in a polymeric network. This value can be calculated from the storage modulus at a particular temperature by using Equation 1, where E' is the storage modulus obtained from DMA, R denotes the universal gas constant, and T is the temperature.

$$\rho = \frac{E'}{3RT}. \quad (1)$$

The crosslinking densities at 180°C for all the vitrimeric systems investigated herein are shown in Table 3 along with MFI at 190°C. A higher crosslinking density corresponds to a higher mechanical strength up to a certain level. The maximum crosslinking density was observed for MA_2DM_2, which was found to be 3.52×10^{-5} mol cm^{-3} and this crosslinking density is almost double compared with that of MA_2 which has a crosslinking density of 1.81×10^{-5} mol cm^{-3}. It can be observed that the average crosslinking density is around 1.5×10^{-5} mol cm^{-3} for the 0.5 and 1 wt% samples without any significant increase in the crosslinking density when DM was added. In contrast, there was a substantial increase in crosslinking density for the MA_2DM_2 system as compared with the MA_2 system. Notably, the value of the crosslinking density almost doubled, thus suggesting that a rigid polymeric network existed at the core. Similar observations can be made from the MFR data. MFR

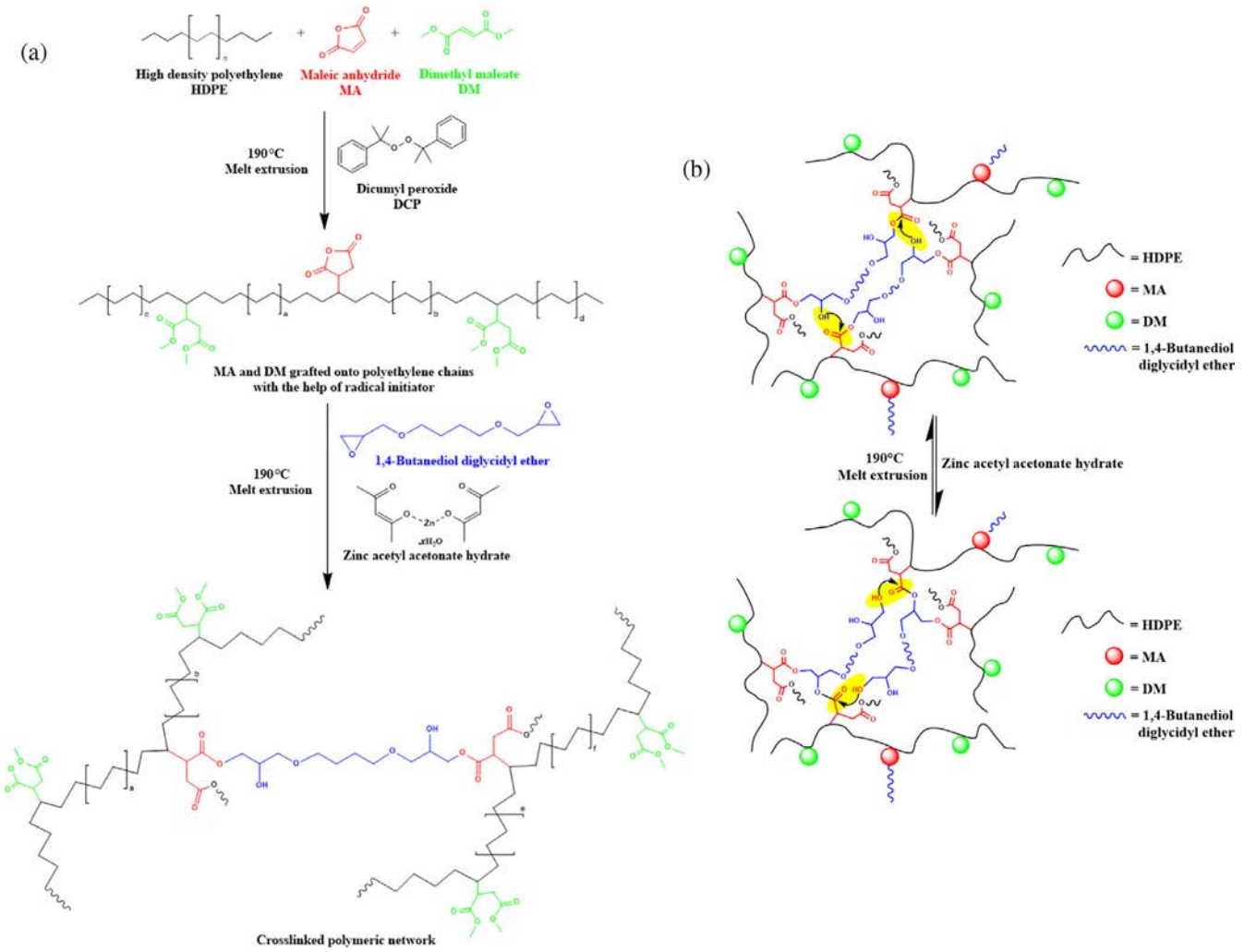

FIGURE 1 (a) HDPE backbone subjected to grafting with MA and DM and subsequent crosslinking with 1,4-butanediol diglycidyl ether to create a vitrimeric 3D network system. (b) Schematic illustration of the exchange reaction site depicting the transesterification reaction. [Color figure can be viewed at wileyonlinelibrary.com]

decreases due to crosslinking in the samples and there is significant decrease in MFR for 2 wt% due to extensive crosslinking. To prove that DM is not providing any crosslinking, we tested the DM_1 system without MA and found that the polymer damped in the same way as HDPE after the melting temperature had been reached (Figure 2d). There is a small plateau beyond 140°C, but the sample melts completely, indicating DM does not participate in any meaningful crosslinking. The higher crosslinking density was also apparent from changes in the torque while processing the polymer in DSM. In particular, the torque increased from 30 to 40 N m with a higher crosslinking density, which made the processing of the MA_2DM_2 system difficult. This is also a good indication of higher MA grafting density in the case of MA_2DM_2 as compared with the MA_2 system, based on the consideration that DM is not a reactive grafting agent and does not take part in the formation of a networked structure. The crosslinking density did not increase significantly in the systems with MA and DM contents of 0.5 and 1 wt%. This might be due to the smaller amount of MA added to the system. On the other hand, we could not melt-process vitrimers with MA and DM contents higher than 2 wt% due to the excessive torque that was reached in these cases.

To confirm the role of DM as a surface modifier rather than a crosslinking agent, 2MA-HDPE and 2MA2DM-HDPE were prepared. 2MA-HDPE is grafted with 2 wt% MA, while 2MA2DM-HDPE was prepared using both 2 wt% MA and 2 wt% DM grafted onto HDPE. SEs for these samples were calculated using the contact angle measurement technique by employing water to get the polar component and diiodomethane to get the dispersive component of the SE. It was observed that the

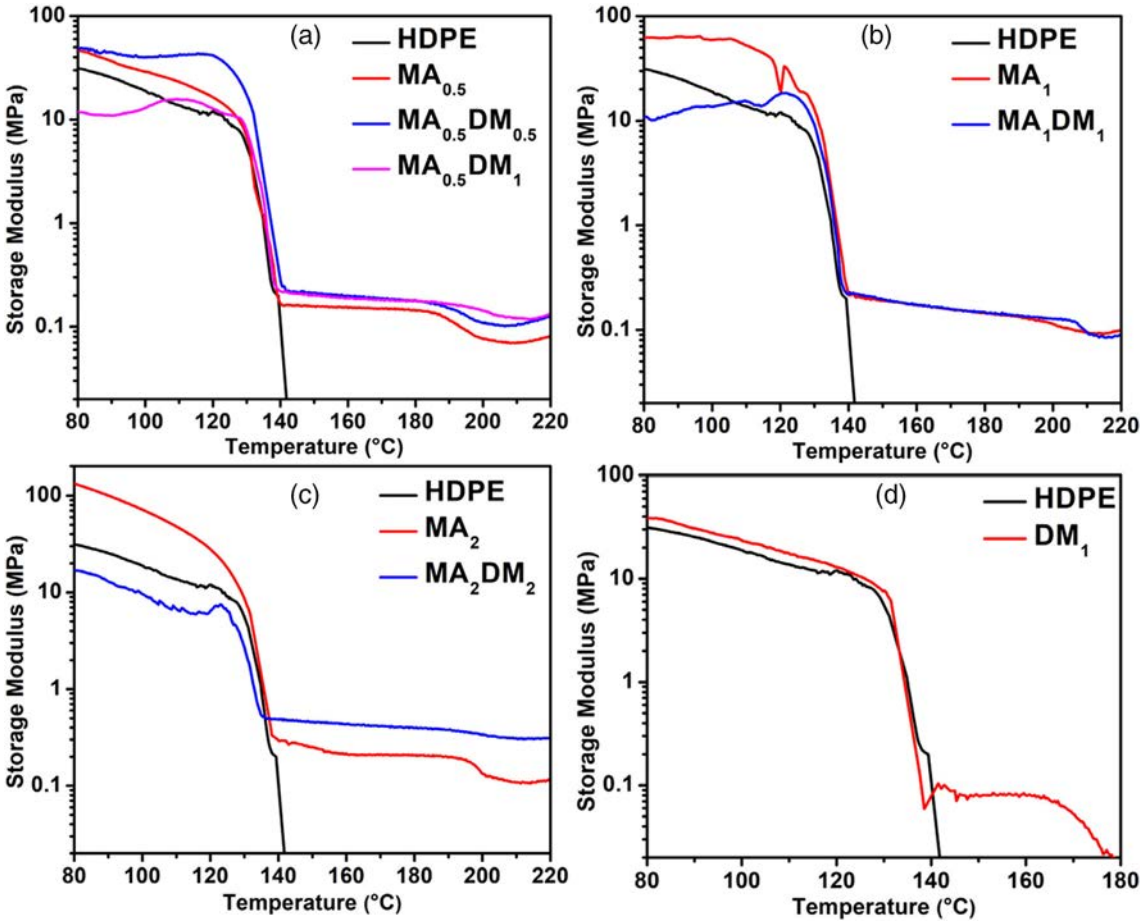

FIGURE 2 Storage modulus versus temperature plots for vitrimeric systems with maleic anhydride (MA) and dimethyl maleate (DM) contents of 0.5 wt% (a), 1 wt% (b), and 2 wt% (c), respectively. The rubbery plateau suggests the formation of a crosslinked network. The crosslinking density increased with increasing the grafting density. DM_1 without MA (d) does not participate in crosslinking and thus behaves like high-density polyethylene (HDPE) and melts completely at 150°C. [Color figure can be viewed at wileyonlinelibrary.com]

TABLE 3 The values of crosslinking density of high-density polyethylene (HDPE) vitrimer-based materials were obtained from dynamic mechanical analysis along with their melt flow rates.

Sample code	E' at 453.15 K (MPa)	Crosslinking density ν ($\times 10^{-5}$ mol cm^{-3})	Melt flow rate (MFR) at 463.15 K (g/10 min)
HDPE	0.00	0.00	9.015 ± 0.470
$MA_{0.5}$	0.15	1.29	0.524 ± 0.028
$MA_{0.5}DM_{0.5}$	0.18	1.59	0.591 ± 0.021
$MA_{0.5}DM_1$	0.18	1.58	0.619 ± 0.014
MA_1	0.15	1.29	0.535 ± 0.009
MA_1DM_1	0.15	1.30	0.509 ± 0.008
MA_2	0.21	1.83	0.116 ± 0.007
MA_2DM_2	0.40	3.52	-

Abbreviations: DM, dimethyl maleate; MA, maleic anhydride.

water contact angle first reduced to 74.1° for 2MA-HDPE owing to the polar nature of MA and then the water contact angle increased to 80.8° due to the two nonpolar methyl groups of the DM (Figure 3). It should be noted that the SEs were measured at room temperature while the grafting was performed in melts.

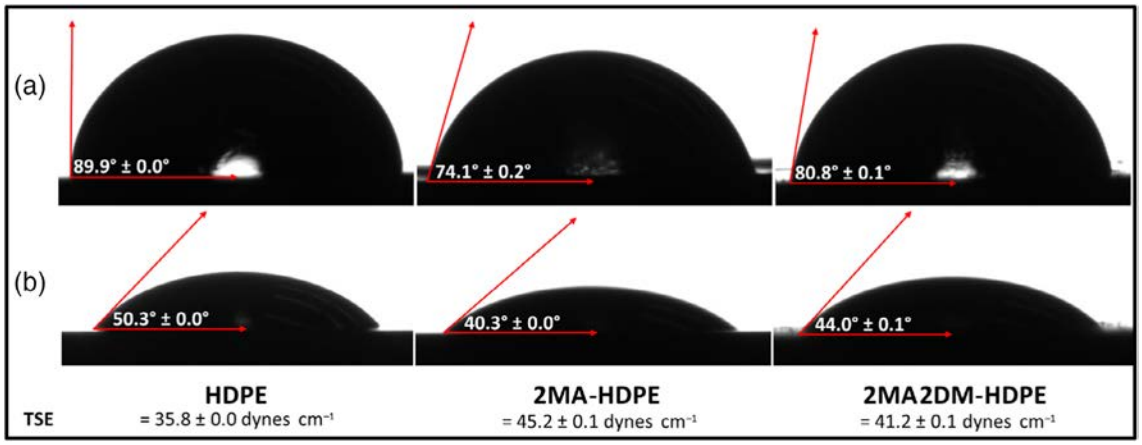

FIGURE 3 (a) Water droplet images and their contact angles on HDPE, 2MA-HDPE, and 2MA2DM-HDPE, respectively. (b) Diiodomethane droplet images and their contact angles on HDPE, 2MA-HDPE, and 2MA2DM-HDPE, respectively. DM, dimethyl maleate; HDPE, high-density polyethylene; MA, maleic anhydride; TSE, total surface energy. [Color figure can be viewed at wileyonlinelibrary.com]

TABLE 4 Contact angle measurements for three samples to understand the role of DM in reducing the surface energy of polymer for better grafting of MA onto HDPE.

Sample	Contact angle in water	Contact angle in diiodomethane	Polar component of SE (dynes cm^{-1})	Dispersive component of SE (dynes cm^{-1})	Total SE (dynes cm^{-1})
HDPE	89.9° ± 0.0°	50.3° ± 0.0°	1.7 ± 0.0	34.1 ± 0.0	35.8 ± 0.0
2MA-HDPE	74.1° ± 0.2°	40.3° ± 0.0°	5.7 ± 0.1	39.5 ± 0.0	45.2 ± 0.1
2MA2DM-HDPE	80.8° ± 0.1°	44.0° ± 0.1°	3.6 ± 0.1	37.6 ± 0.0	41.2 ± 0.1

Abbreviations: DM, dimethyl maleate; HDPE, high-density polyethylene; MA, maleic anhydride; SE, surface energy.

It is evident that DM grafting reduced TSE of MA-grafted HDPE as confirmed by the contact angles and the SEs shown in Table 4. For example, the addition of 2 wt% MA increased the SE from 35.8 to 44.2 dynes cm^{-1}, while the addition of 2 wt% DM along with 2% MA decreased the TSE to 41.2 dynes cm^{-1}. The SE values were further confirmed using Dyne Test Inks. With four dyne levels available and applying the Dyne Ink Pen methodology, HDPE's SE was less than 38 dynes cm^{-1} and 2MA-HDPE's SE was higher than 44 dynes cm^{-1}, while 2MA2DM-HDPE had a lower SE below 42 dynes cm^{-1}.

To understand any phase separation, we performed SEM with a magnification of 5000× (Figure 4). The fractured surfaces SEM analysis shows that both HDPE and 2MA2DM-HDPE samples have essentially similar features, without any phase separation. On the contrary, MA addition to HDPE shows some bright domains presumably formed by some phase-separated 2MA-HDPE domains. Further investigations are required to understand this phase separation in more detail.

FTIR spectroscopy was employed to further characterize the grafting of MA and DM onto HDPE, and the spectrum of $MA_{0.5}DM_{0.5}$ is shown in Figure 5. The peaks around 1740 cm^{-1} correspond to the C═O stretching vibration of ester linkages. Its peak intensity with respect to HDPE's —CH_2— rocking peaks at 730 and 720 cm^{-1} indicate how much MA has been grafted and crosslinked. The intensity of the 1740 cm^{-1} peak in the FTIR spectrum of $MA_{0.5}DM_{0.5}$ is higher as compared with that of $MA_{0.5}$, thus suggesting more grafting of MA had been achieved with the help thanks to DM lowering the SE of maleated HDPE (Figure S1A). Meanwhile, the peak observed at 1620 cm^{-1} in the FTIR spectrum of $MA_{0.5}DM_{0.5}$ exclusively corresponds to the C═O stretching vibration for DM that are absent for $MA_{0.5}$. The peaks appearing around 1250 cm^{-1} correspond to the C—C—O stretching vibration of the glycidyl ether, which forms the crosslinking. Weak O—H stretching could also be observed, indicating that free alcohol groups were available for the transesterification reaction. Meanwhile, the stronger peaks at 2919 and 2850 cm^{-1}, respectively correspond to asymmetric and symmetric —CH_2— stretching vibrations for HDPE. All these findings clearly suggest that the HDPE had indeed underwent grafting and vitrimer formation. The ester peaks are weaker because of the lower grafting density.

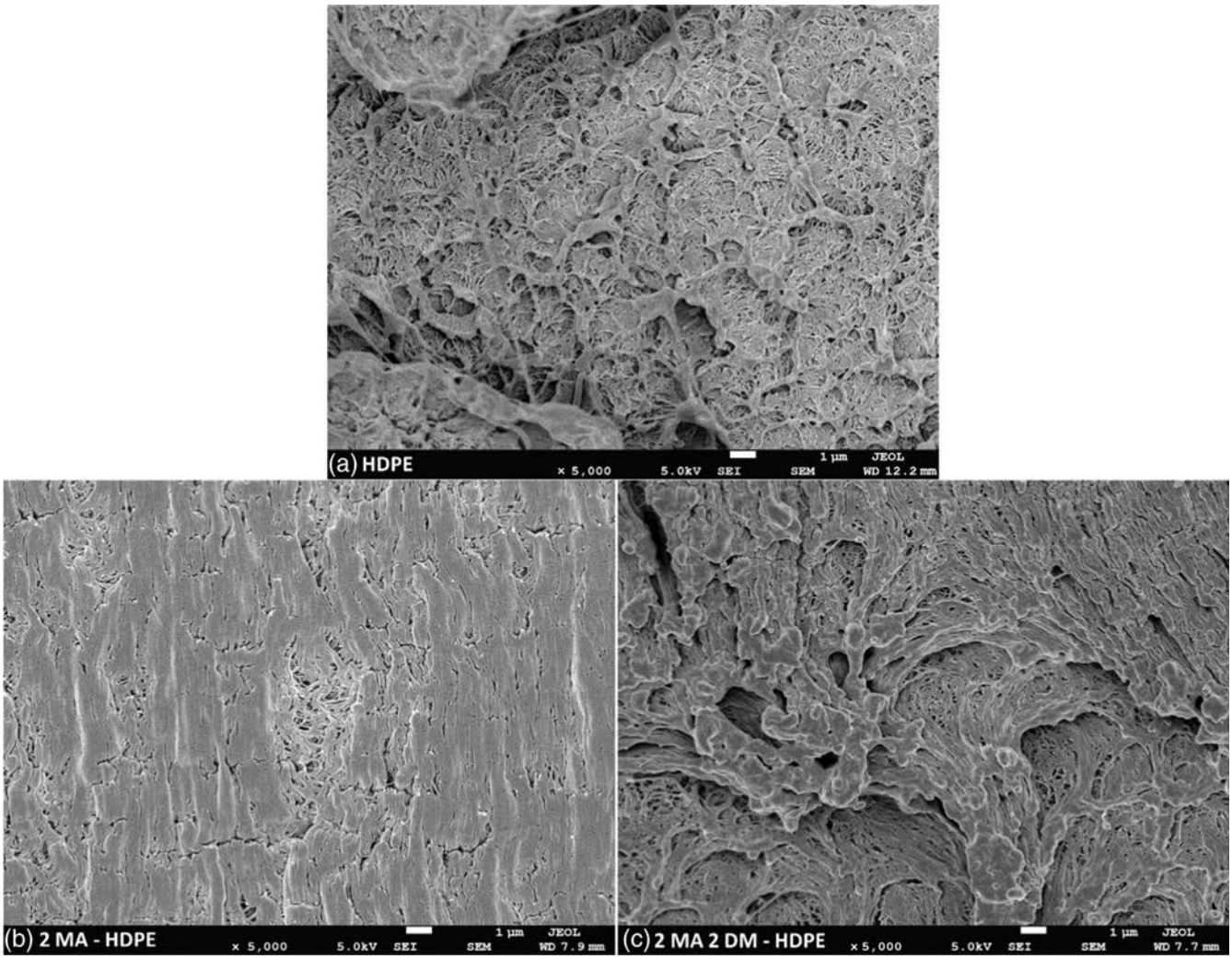

FIGURE 4 SEM images of (a) HDPE, (b) 2MA-HDPE, and (c) 2MA2DM-HDPE (magnification 5000×). DM, dimethyl maleate; HDPE, high-density polyethylene; MA, maleic anhydride.

Next, we wanted to study how vitrimer formation would affect the crystallinity of the polymer by employing DSC. In this study, heating cycles were performed two times—the first heating cycle was employed to erase the thermal history of the sample and the second heating cycle was performed to measure the melting temperature and percentage crystallinity of the vitrimers. A cooling cycle was also performed to measure the temperature of crystallization. Heating and cooling cycles for 0.5, 1, and 2 wt% systems are shown in Figure 6. The heat of fusion was determined by using a linear baseline. The degree of crystallinity (%) of vitrimers was calculated from the ratio of the experimentally determined melt enthalpy (ΔH_m) and the theoretical melt enthalpy of a 100% crystalline polyethylene (ΔH_{mo} 293.6 J g^{-1}) using Equation (2).

$$\text{Percentage crystallinity}\,\chi_c = \frac{\Delta H_m}{\Delta H_{m0}} \times 100. \qquad (2)$$

The parameters such as the enthalpy of melting ΔH_m, enthalpy of crystallization ΔH_c, percentage crystallinity χ_c, melting temperature T_m, and crystallization temperature T_c obtained from DSC are tabulated in Table 5. The melting and cooling curves have broadened as compared to control HDPE. Crystallinity decreases as grafting is increased because MA and DM hinder chain packaging. In addition, crosslinking also reduces crystallinity because it lowers the chain mobility, thus preventing the chains from packing into ordered crystalline arrangements. Accordingly, the enthalpies of melting and crystallization also decrease. Broad heating and cooling curves indicate that these crosslinks are well distributed, and maybe there are differences in crystallite size distribution in the polymer, because of heterogeneous crosslinking.

The mechanical properties of these systems such as the tensile stress at yield and break, Young's modulus,

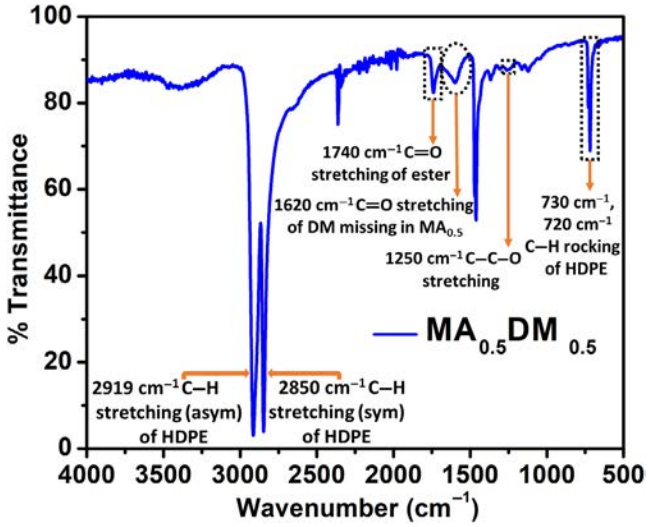

FIGURE 5 FTIR spectrum of $MA_{0.5}DM_{0.5}$. Peaks corresponding to ester C═O stretching and C—C—O stretching for a crosslinked network were observed. The stronger peaks correspond to HDPE —CH_2— stretching and rocking vibrations. DM, dimethyl maleate; HDPE, high-density polyethylene; MA, maleic anhydride. [Color figure can be viewed at wileyonlinelibrary.com]

and elongation at break percentage were also investigated. These values are shown in Figure 7 and Table 6 along with the standard deviations. There are two important factors that play contrasting roles. A decrease in the crystallinity of the polymer leads to a decrease in the tensile strength and modulus, while an increase in the crosslinking density leads to an increase in the tensile strength and modulus. Recently, Montoya and coworkers showed a decrease in tensile stress at yield and break for their vitrimeric systems generated from LDPE.[31] The vitrimers described in this study retain the elastic behavior of HDPE and later show higher strength in the plastic region owing to the networked structure. HDPE showed much elongation because of the free polymer chain slippage due to their uncrosslinked structure. In contrast, the vitrimers are crosslinked and their polymer chains cannot slide, and thus they break at a lower elongation percentage. Overall, these vitrimers behave elastically when small stress is applied but have enhanced mechanical properties when higher stress is applied, and thus they exhibit some properties of thermosets that can be later improved.

The toughness of the material was tested on notched samples. Usually, impact resistance decreases with an increase in crystallinity and increases with crosslinking density although the impact strength declines beyond a certain crosslinking degree. The results observed for our systems are shown in Figure 8. It is observed that both crosslinking and crystallinity significantly influence the impact strength. MA_2, which had the lowest crystallinity and highest crosslinking density, exhibited a ~2.8-fold increase relative to the control sample (unmodified HDPE).

We also performed repeated melt-processing experiments with MA_1DM_1. For reprocessing, the samples were cut into small pieces and subsequently fed into the extruder at 190°C for 4 min to generate samples for testing. All these properties are readily retained while these materials are also melt-reprocessable, unlike thermosets. For instance, two reprocessing cycles of MA_1DM_1 are shown in Figure 9a, where MA_1DM_1 was melt-reprocessed at 190°C and then molded into dumbbells and rectangular samples for further testing. Figure 9b shows the storage modulus data for HDPE, MA_1DM_1, MA_1DM_1-Reprocessed 1 (with one reprocessing cycle), and MA_1DM_1-Reprocessed 2 (with two reprocessing cycles). Overall, there was no decline in the storage modulus. Rather, the storage modulus increased following the first reprocessing cycle and then decreased after the second reprocessing cycle. This suggests that there is further crosslinking that happened in the first cycle of reprocessing. In the second reprocessing, a few crosslinks might have degraded as observed in the form of mild darkening (Figure 9a) resulting in a decrease in crosslinking.

The tensile properties of these reprocessed samples are tabulated in Table 7. The tensile stress at yield decreases with each processing cycle. The modulus elongation at break decreased following the first reprocessing cycle, indicating further crosslink formation, which was also evident in the storage modulus data. This finding further indicates that the crosslinks are disoriented, thereby making the material less crystalline so that less stress is required for the strain and break. Following the second reprocessing cycle, the tensile stress at break of the MA_1DM_1-Reprocessed 2 sample had diminished to a similar value as that exhibited by HDPE. Also, modulus and break elongation increased indicating that the extent of exchange transesterification had been reduced, possibly due to catalyst leaching. All these findings demonstrate that these HDPE-based vitrimers retained their mechanical integrity even after they have been subjected to two processing cycles. Thus, this strategy has the potential to offer a robust approach for making durable and reprocessable vitrimers that will be suitable for many practical applications.

Finally, to prove that the transesterification exchange reaction that takes place to make these vitrimers reprocessable, stress relaxation experiments were performed on $MA_{0.5}DM_{0.5}$ sample. Normalized relaxation modulus as a function of time were performed at different temperatures ranging from 145 to 165°C as shown in Figure 10a. According to Maxwell behavior, τ was calculated for each

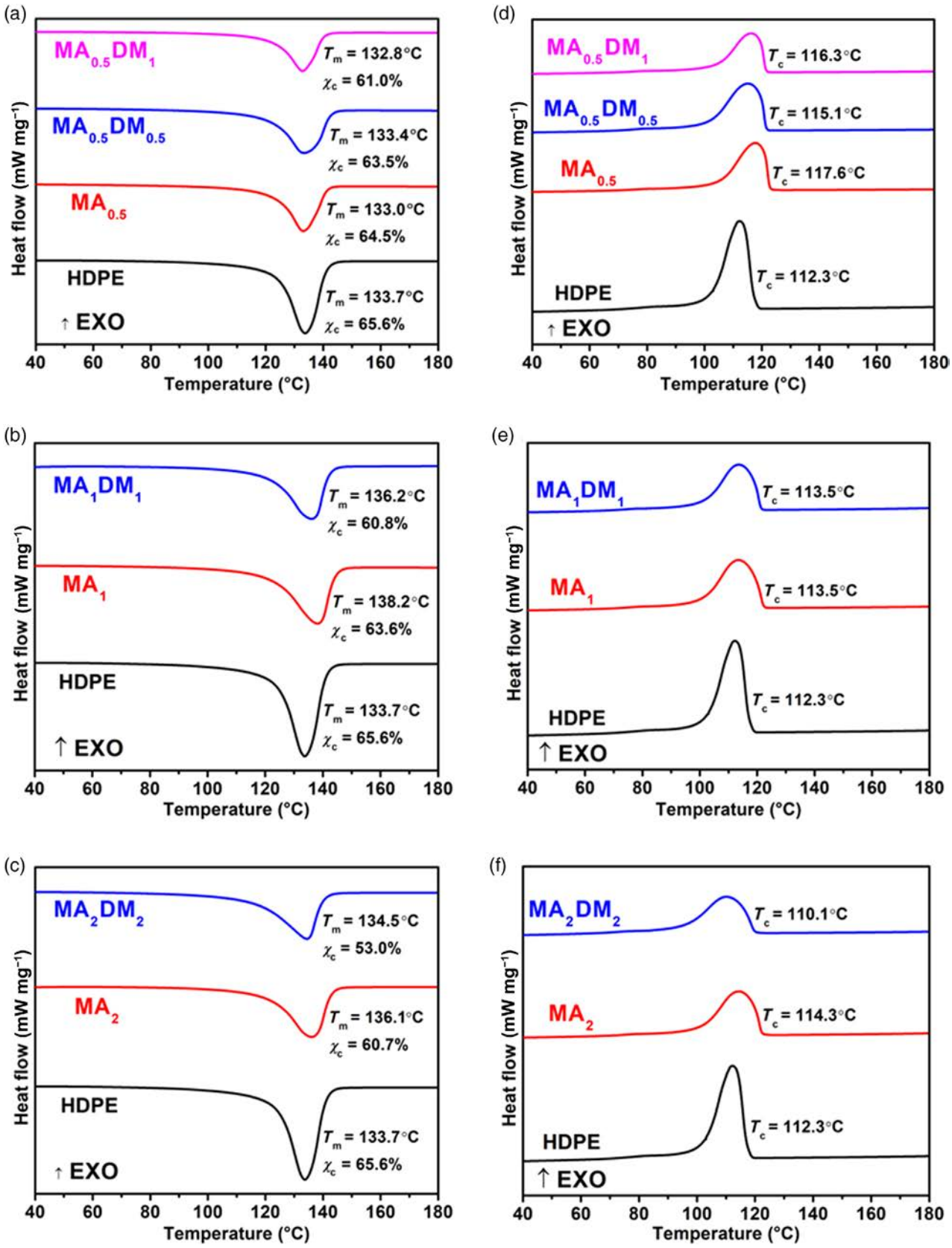

FIGURE 6 Differential scanning calorimetry (DSC) heating curves for: (a) 0.5 wt%, (b) 1 wt%, and (c) 2 wt% systems, respectively, with melting temperatures and percentage crystallization decreasing with increasing grafting densities DSC cooling curves for: (d) 0.5 wt%, (e) 1 wt%, and (f) 2 wt% systems, respectively, with crystallization temperature. DM, dimethyl maleate; HDPE, high-density polyethylene; MA, maleic anhydride. [Color figure can be viewed at wileyonlinelibrary.com]

Sample	ΔH_m (J g^{-1})	ΔH_c (J g^{-1})	χ_c (%)	T_m (°C)	T_c (°C)
HDPE	192.5	205.8	65.6	133.7	112.3
$MA_{0.5}$	189.5	204.0	64.5	133.0	117.6
$MA_{0.5}DM_{0.5}$	186.3	191.6	63.5	133.4	115.1
$MA_{0.5}DM_1$	179.2	188.6	61.0	132.8	116.3
MA_1	186.8	199.2	63.6	138.2	113.5
MA_1DM_1	178.4	181.6	60.8	136.2	113.5
MA_2	178.1	185.0	60.7	136.1	114.3
MA_2DM_2	155.5	159.4	53.0	134.5	110.1

Abbreviations: DM, dimethyl maleate; HDPE, high-density polyethylene; MA, maleic anhydride.

TABLE 5 Enthalpy of melting ΔH_m, enthalpy of crystallization ΔH_c, percentage crystallinity χ_c, melting temperature T_m, and crystallization temperature T_c values obtained via DSC.

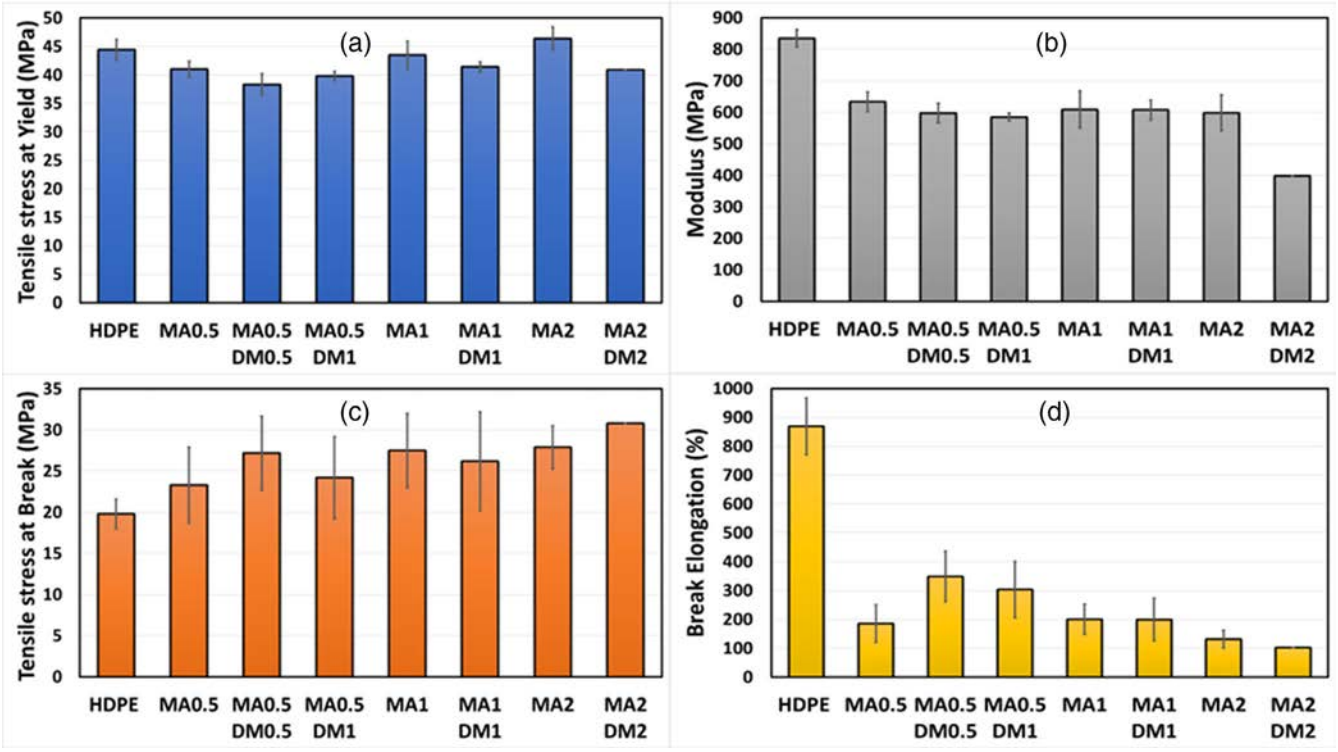

FIGURE 7 Various graphs including (a) tensile stress at yield, (b) modulus, (c) tensile stress at break, and (d) break elongation percentage of samples used in this study. Crosslinking decreases the break elongation and modulus but improves the tensile stress at break. DM, dimethyl maleate; HDPE, high-density polyethylene; MA, maleic anhydride. [Color figure can be viewed at wileyonlinelibrary.com]

TABLE 6 Tensile stress at yield, modulus, tensile stress at break, break elongation percentage, and impact strength of samples used in this study with standard deviation.

Sample	Tensile stress at yield (MPa)	Tensile stress at break (MPa)	Modulus (MPa)	Break elongation (%)	Impact strength (kJ m^{-2})
HDPE	44.4 ± 1.8	19.8 ± 1.8	835 ± 28	868.9 ± 98.7	6.4 ± 0.7
$MA_{0.5}$	41.0 ± 1.4	23.3 ± 4.6	633 ± 31	185.3 ± 65.4	15.7 ± 5.4
$MA_{0.5}DM_{0.5}$	38.3 ± 1.9	27.2 ± 4.5	597 ± 31	349.2 ± 87.2	9.8 ± 2.9
$MA_{0.5}DM_1$	39.8 ± 0.8	24.2 ± 5.0	585 ± 12	303.2 ± 97.6	11.8 ± 0.8
MA_1	43.5 ± 2.4	27.5 ± 4.5	609 ± 59	200.8 ± 52.6	13.8 ± 1.4
MA_1DM_1	41.4 ± 0.9	26.2 ± 6.0	607 ± 32	199.4 ± 73.5	10.8 ± 1.9
MA_2	46.4 ± 2.0	27.9 ± 2.6	598 ± 57	131.4 ± 30.2	18.2 ± 2.8
MA_2DM_2	40.9[a]	30.8[a]	398[a]	102.3[a]	Not tested

[a]Indicates that only one sample was used.

temperature as the time required for the relaxation modulus to decrease to $1/e$ (36.8%) of its initial value. This τ is related to activation energy of exchange reaction for the vitrimer following an Arrhenius relationship by Equation (3):

$$\tau = \tau_0 e^{-\frac{E_a}{RT}}, \quad (3)$$

where R is the gas constant, T is the temperature and τ_0 is pre-exponential factor.

The activation energy for transesterification reaction was evaluated from the slope of $\ln(\tau)$ versus $1/T$ graph and found to be 59 kJ mol^{-1} **(**Figure 10b**)**. The relaxation times for the vitrimeric samples are extremely fast. For instance, after 5% strain applied, $MA_{0.5}DM_{0.5}$ relaxes to 36.8% of its initial value in 2.17 s at 145°C and 1.25 s at 160°C. These fast relaxation times indicate highly efficient rearrangement of the polymer chains and fast transesterification exchanges involved at the core of these vitrimers.[37] There have been numerous reports in literature for the activation energies for transesterification chemistries ranging from 40 to 170 kJ mol^{-1} involving different catalysts like PPh_3, $Zn(OAc)_2$ TBD, TCA, Triflic acid, Dibutyltin(acac)$_2$, and so forth.[5,38,39] This clearly proves that transesterification involving zinc acetylacetonate is quite fast as compared to different catalysts. The stress relaxation experiments also prove that the product of this study is a vitrimer involving exchange reactions rather than nonprocessable crosslinked HDPE by DCP.

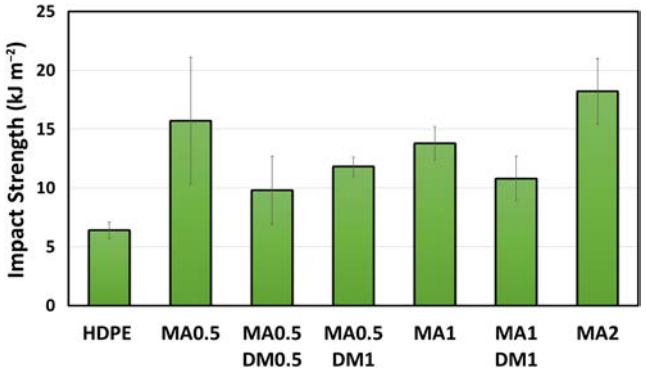

FIGURE 8 Variation of impact strength for the vitrimers generated from HDPE. Crosslinking plays an important role and increases the impact strength of the material. DM, dimethyl maleate; HDPE, high-density polyethylene; MA, maleic anhydride. [Color figure can be viewed at wileyonlinelibrary.com]

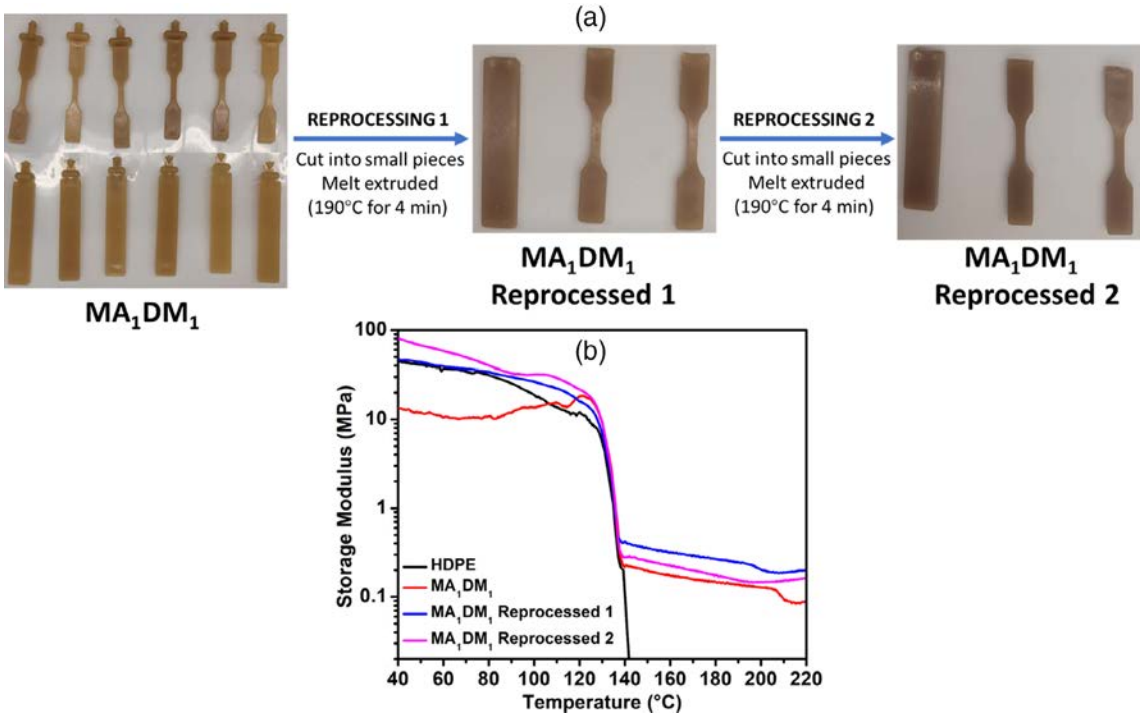

FIGURE 9 (a) Photographs of MA_1DM_1, which were taken before (left) and after (right) the samples had underwent two reprocessing cycles. A mild darkening phenomenon is visible after the reprocessing cycles. (b) Storage modulus data for HDPE, MA_1DM_1, MA_1DM_1-Reprocessed 1, and MA_1DM_1-Reprocessed 2 samples. The storage modulus does not decrease for the reprocessed samples, indicating that crosslinking is maintained. DM, dimethyl maleate; HDPE, high-density polyethylene; MA, maleic anhydride. [Color figure can be viewed at wileyonlinelibrary.com]

TABLE 7 Tensile properties for HDPE, MA_1DM_1, MA_1DM_1-Reprocessed 1, and MA_1DM_1-Reprocessed 2 samples.

Sample code	Tensile stress at yield (MPa)	Tensile stress at break (MPa)	Modulus (MPa)	Break elongation (%)
HDPE	44.4 ± 1.8	19.8 ± 1.8	835 ± 28	868.9 ± 98.7
MA_1DM_1	41.4 ± 0.9	26.2 ± 6.0	607 ± 32	199.4 ± 73.5
MA_1DM_1-Reprocessed 1	38.9 ± 2.3	22.6 ± 2.4	491 ± 50	132.1 ± 10.2
MA_1DM_1-Reprocessed 2	37.5 ± 1.3	21.8 ± 3.0	578 ± 33	168.1 ± 48.4

Abbreviations: DM, dimethyl maleate; HDPE, high-density polyethylene; MA, maleic anhydride.

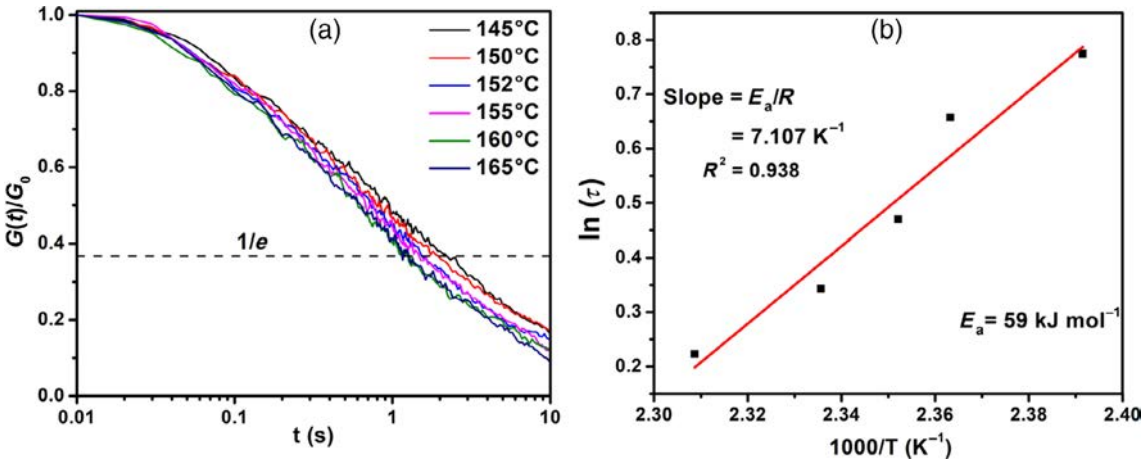

FIGURE 10 (a) Normalized stress relaxation curves of $MA_{0.5}DM_{0.5}$ vitrimer. The τ values were calculated using $1/e$ of the relaxation modulus. (b) Arrhenius plots for $\ln(\tau)$ versus $1000/T$ and a linear fit to calculate the activation energy ($E_a = 59$ kJ mol^{-1}). [Color figure can be viewed at wileyonlinelibrary.com]

4 | CONCLUSION

We have demonstrated a solvent-free and continuous approach to produce HDPE-based vitrimers. The interplay of the two grafting agents is an important aspect of this study because MA acted as a reactive grafting agent that aided in crosslinking while DM served as a coagent, which helped to lower the SE, thereby facilitating the grafting of MA to HDPE. Significant enhancement in tensile stress at break was observed for our HDPE-based vitrimers, while the tensile stress at yield was similar to that of unmodified HDPE. The impact resistance also improved as the crosslinking density increased and, in some cases, increased by 2.8 times compared with the neat HDPE. Although the elongation at break percentage has decreased due to crosslinking but these materials have a superiority when it comes to toughness as evident from the high impact strength. Storage modulus beyond the T_m confirmed the presence of a crosslinked network. The crosslinking density increased twofold for MA_2DM_2 as compared with MA_2 because of the better grafting of MA thanks to the lower SE provided by DM. Crystallinity decreased as the crosslinking and grafting increased. Our HDPE vitrimers have even greater thermal stability than HDPE itself. Extremely fast relaxation times indicated rapid transesterification exchange reactions with an activation energy of 59 kJ mol^{-1} catalyzed by the zinc acetylacetonate. Overall, this strategy has the potential to offer a robust approach for the production of durable and reprocessable vitrimers that will be suitable for many practical applications.

AUTHOR CONTRIBUTIONS

Subhaprad Ash: Conceptualization (equal); formal analysis (lead); investigation (lead); methodology (lead); project administration (lead); validation (lead); writing – original draft (lead). **Rishi Sharma:** Investigation (supporting); supervision (supporting). **Muhammad Naveed:** Project administration (supporting). **Muhammad Rabnawaz:** Conceptualization (equal); funding acquisition (lead); resources (lead); supervision (lead). **Shalin Patil:** Data curation (supporting). **Shiwang Cheng:** Data curation (supporting).

ACKNOWLEDGMENTS

This publication was developed under Award Number: 2044877 awarded by the U.S. National Science Foundation (NSF) to Michigan State University. It has not been formally reviewed by NSF. The views expressed in this document are solely those of the authors and do not necessarily reflect those of the Agency. NSF does not endorse any products or commercial services mentioned in this publication.

CONFLICT OF INTEREST STATEMENT

The authors declare no conflicts of interest.

DATA AVAILABILITY STATEMENT

The data that support the findings of this study are available upon request from the corresponding author.

ORCID

Subhaprad Ash https://orcid.org/0000-0002-3816-1139
Muhammad Rabnawaz https://orcid.org/0000-0002-4576-1810

REFERENCES

[1] N. Singh, D. Hui, R. Singh, I. P. S. Ahuja, L. Feo, F. Fraternali, *Compos. B Eng.* **2017**, *115*, 409.
[2] M. Rabnawaz, I. Wyman, R. Auras, S. Cheng, *Green Chem.* **2017**, *19*, 4737.
[3] H. Ahmad, D. Rodrigue, *Polym. Eng. Sci.* **2022**, *62*, 2376.
[4] M. Capelot, D. Montarnal, F. Tournilhac, L. Leibler, *J. Am. Chem. Soc.* **2012**, *134*, 7664.
[5] M. Capelot, M. M. Unterlass, F. Tournilhac, L. Leibler, *ACS Macro Lett.* **2012**, *1*, 789.
[6] X. Chen, L. Li, K. Jin, J. M. Torkelson, *Polym. Chem.* **2017**, *8*, 6349.
[7] Y.-X. Lu, Z. Guan, *J. Am. Chem. Soc.* **2012**, *134*, 14226.
[8] Y.-X. Lu, F. Tournilhac, L. Leibler, Z. Guan, *J. Am. Chem. Soc.* **2012**, *134*, 8424.
[9] P. Taynton, C. Zhu, S. Loob, R. Shoemaker, J. Pritchard, Y. Jin, W. Zhang, *Polym. Chem.* **2016**, *7*, 7052.
[10] N. Zheng, Z. Fang, W. Zou, Q. Zhao, T. Xie, *Angew. Chem., Int. Ed.* **2016**, *55*, 11304.
[11] P. Zheng, T. J. McCarthy, *J. Am. Chem. Soc.* **2024**, *2012*, 134.
[12] W. Schmolke, N. Perner, S. Seiffert, *Macromolecules* **2015**, *48*, 8781.
[13] Y. Nishimura, J. Chung, H. Muradyan, Z. Guan, *J. Am. Chem. Soc.* **2017**, *139*, 14881.
[14] S. Nevejans, N. Ballard, J. I. Miranda, B. Reck, J. M. Asua, *Phys. Chem. Chem. Phys.* **2016**, *18*, 27577.
[15] J. N. Cambre, B. S. Sumerlin, *Polymer* **2011**, *52*, 4631.
[16] C. C. Deng, W. L. A. Brooks, K. A. Abboud, B. S. Sumerlin, *ACS Macro Lett.* **2015**, *4*, 220.
[17] C. J. Kloxin, T. F. Scott, B. J. Adzima, C. N. Bowman, *Macromolecules* **2010**, *43*, 2643.
[18] C. N. Bowman, C. J. Kloxin, *Angew. Chem. Int. Ed.* **2012**, *51*, 4272.
[19] C. J. Kloxin, C. N. Bowman, *Chem. Soc. Rev.* **2013**, *42*, 7161.
[20] C. Zhang, Z. Yang, N. T. Duong, X. Li, Y. Nishiyama, Q. Wu, R. Zhang, P. Sun, *Macromolecules* **2019**, *52*, 5014.
[21] T. F. Scott, A. D. Schneider, W. D. Cook, C. N. Bowman, *Science* **2005**, *308*, 1615.
[22] X. Chen, M. A. Dam, K. Ono, A. Mal, H. Shen, S. R. Nutt, K. Sheran, F. Wudl, *Science* **2002**, *295*, 1698.
[23] D. Montarnal, M. Capelot, F. Tournilhac, L. Leibler, *Science* **2011**, *334*, 965.
[24] C. A. Angell, *Science* **1995**, *267*, 1924.
[25] M. Röttger, T. Domenech, R. van der Weegen, A. Breuillac, R. Nicolaÿ, L. Leibler, *Science* **2017**, *356*, 62.
[26] G. P. Kar, M. O. Saed, E. M. Terentjev, *J. Mater. Chem. A* **2020**, *8*, 24137.
[27] N. J. Van Zee, R. Nicolaÿ, *Prog. Polym. Sci.* **2020**, *104*, 101233.
[28] M. Maaz, A. Riba-Bremerch, C. Guibert, N. J. Van Zee, R. Nicolaÿ, *Macromolecules* **2021**, *54*, 2213.
[29] M. C. Montoya-Ospina, H. Verhoogt, T. A. Osswald, *SPE Polym.* **2022**, *3*, 25.
[30] M. C. Montoya-Ospina, J. Zeng, X. Tan, T. A. Osswald, *Polymer* **2023**, *15*, 1332.
[31] M. C. Montoya-Ospina, H. Verhoogt, M. Ordner, X. Tan, T. A. Osswald, *Polym. Eng. Sci.* **2022**, *62*, 4203.
[32] I. Novák, E. Borsig, L. Hrčková, A. Fiedlerová, A. Kleinová, V. Pollák, *Polym. Eng. Sci.* **2007**, *47*, 1207.
[33] P. Ma, L. Jiang, T. Ye, W. Dong, M. Chen, *Polymer* **2014**, *6*, 1528.
[34] DOWLEX™ IP-10 Polyethylene Resin. https://www.dow.com/en-us/pdp.dowlex-ip-10-polyethylene-resin.34286z.html.
[35] ASTM International, *ASTM D638-14, Standard Test Method for Tensile Properties of Plastics*. **2015**.
[36] *Standard Test Methods for Determining the Izod Pendulum Impact Resistance of Plastics*. **2010**.
[37] M. Chen, L. Zhou, Y. Wu, X. Zhao, Y. Zhang, *ACS Macro Lett.* **2019**, *8*, 255.
[38] J. L. Self, N. D. Dolinski, M. S. Zayas, J. Read de Alaniz, C. M. Bates, *ACS Macro Lett.* **2018**, *7*, 817.
[39] W. Liu, D. F. Schmidt, E. Reynaud, *Ind. Eng. Chem. Res.* **2017**, *56*, 2667.

SUPPORTING INFORMATION

Additional supporting information can be found online in the Supporting Information section at the end of this article.

How to cite this article: S. Ash, R. Sharma, M. Naveed, S. Patil, S. Cheng, M. Rabnawaz, *J. Appl. Polym. Sci.* **2024**, *141*(28), e55652. https://doi.org/10.1002/app.55652